Triggered Transience of Plastic Materials by a Single Electron Transfer Mechanism

Adam M. Feinberg, †,1,2 Oleg Davydovich, †,1,2 Evan M. Lloyd, 1,3 Douglas G. Ivanoff, 1,4 Bethany Shiang, 4 Nancy R. Sottos, 1,4 and Jeffrey S. Moore*,1,2,4

† Denotes equal contribution

¹ Beckman Institute for Advanced Science and Technology, ² Department of Chemistry, ³ Department of Chemical and Biomolecular Engineering, ⁴ Department of Materials Science and Engineering, University of Illinois at Urbana-Champaign, Urbana, Illinois 61801, United States

Abstract

Transient polymers rapidly and controllably depolymerize in response to a specific trigger typically by a chain-end unzipping mechanism. Triggers, such as heat, light, and chemical stimuli, are generally dependent on the chemistry of the polymer backbone or end groups. Single electron transfer (SET), in contrast to other triggering mechanisms, is achievable by various means including chemical, electrochemical, and photochemical oxidation or reduction. Here, we identify SET and subsequent mesolytic cleavage as the major thermal triggering mechanism of cyclic poly(phthalaldehyde) (cPPA) depolymerization. Multimodal SET triggering is demonstrated by both chemical and photoredox triggered depolymerization of cPPA. Redox-active small molecules (*p*-chloranil and 1,3,5-trimethoxybenzene) were used to tune the depolymerization onset temperature of cPPA over a range of 105-135 °C. Extending this mechanism to photoredox catalysis, *N*-methylacridinium hexafluorophosphate (NMAPF₆) was used to photochemically degrade cPPA in solution and thin films. Finally, we fabricated photodegradable cPPA monoliths with a storage modulus of 1.8 GPa and demonstrated complete depolymerization within 25 minutes of sunlight exposure. Sunlight triggered depolymerization of cPPA is demonstrated and potentially useful for the manufacture of

transient devices that vanish leaving little or no trace. Most importantly, this new mechanism is likely to inspire other SET-triggered transient polymers, whose development may address the ongoing crisis of plastic pollution.

Introduction

Synthetic polymers are ubiquitous in our day-to-day lives due to their ease of manufacture¹, wide range of mechanical properties², and resistance to corrosion and aging³. In contrast to polymer production, plastic waste remediation has proven challenging. Synthetic polymers are largely unrecovered at the end of the material lifespan; notably, less than 10% of plastic waste in the U.S. was recycled in 2015, with the remainder largely being sent to landfills (ca. 75%) or burned (ca. 15%). This lack of end-of-life management has resulted in the global plastic pollution crisis.⁴ Transient materials may provide controlled end-of-life strategies for plastic waste mitigation.

The ideal transient material has good mechanical properties, is readily accessible from inexpensive feedstocks, is processable by conventional methods, and is easily tailored to respond to different and orthogonal triggering stimuli. Depolymerization reactions are typically triggered by light⁵, acid⁶, and specific ions⁷, stimuli that are ubiquitious in everyday use. Single electron transfer (SET) triggering of transient polymers presents an alternative route to tunable transient materials. An SET-triggered polymer unzipping reaction offers versatility for materials formulation. Tailored additives would enable SET-triggering from specific light⁸, chemical^{9,10}, or electrical¹¹ input to initiate depolymerization using a single, easily-accessible pathway, shown schematically in Figure 1. In this work, we sought to demonstrate a transient material that is easily synthesized, has a storage modulus of at least 1 GPa, is processable, and is triggered to depolymerize by SET.

A promising transient polymer is cyclic poly(phthalaldehyde) (cPPA), which has a room temperature storage modulus of 1.5-2 GPa¹² and is prepared in a scalable, one-step cationic polymerization reaction from *ortho*-phthalaldehyde (*o*PA), a readily available monomer^{13,14}. cPPA rapidly unzips to form *o*PA on thermal¹⁵, acid¹⁶, or mechanical¹⁷ triggering due to its low ceiling temperature (T_c = -36 °C¹⁸). The mechanisms of acid-triggered¹⁹ and mechanically-triggered¹⁷ cPPA unzipping are well known, but the mechanism of thermal triggering has not been established. While purely ionic and purely radical thermolytic depolymerization mechanisms have been previous proposed²⁰, we hypothesized that SET effectively initiates the unzipping of cPPA by mesolytic cleavage of the radical cation intermediate (**Figure 1**). Here, we present evidence in support of the SET-triggered depolymerization of cPPA and demonstrate the application of this mechanism in the manufacture of sunlight-degradable monolithic materials.

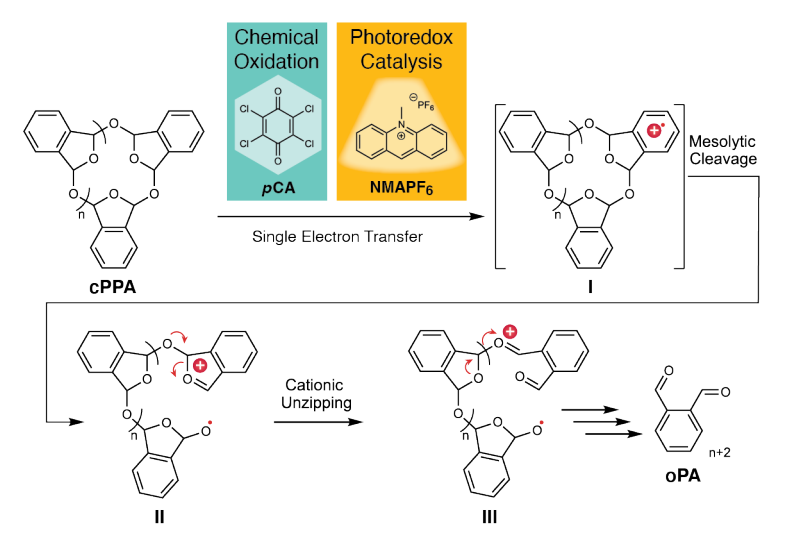


Figure 1. Putative single electron transfer (SET) induced depolymerization of cyclic poly(phthalaldehyde). One electron oxidation of cPPA either via chemical oxidation using p-chloranil (pCA) or photoredox catalysis using N-methylacridinium hexafluorophosphate (NMAPF₆) results in the formation of the corresponding cation radical intermediate I. Following SET activation, mesolytic cleavage of I forms the distonic cation radical II, which is hypothesized to undergo cationic unzipping of the activated oxonium chain end, forming intermediate III, and ultimately the monomer oPA.

Results and Discussion

We hypothesized that, during thermolysis, SET oxidation of cPPA leads to the formation of a benzylic cation radical²¹. Mesolytic fragmentation of the benzylic cation radical^{22,23} is followed by subsequent cationic chain unzipping throughout the polymer chain (**Figure 1**). To test the SET-triggering hypothesis, we first examined the effect of a small molecule oxidant, *p*-chloranil (pCA, E_{red} = -0.005 V vs SCE in acetonitrile²⁴), on cPPA thermal stability (**Figure 2a**). If SET triggers cPPA depolymerization, addition of an oxidant is expected to destabilize the polymer. The addition of pCA resulted in significantly reduced thermal stability, which decreased in a dose-dependent manner. This linear dependence enabled tuning of the thermal degradation onset temperatures over a ca. 15 °C range (0-2 phr (parts per hundred resin) pCA). These results demonstrate that SET is an effective method for triggering cPPA degradation, but do not indicate whether the SET triggering mechanism is operative under typical thermolytic conditions, as SET requires a reductant/oxidant pair. A plausible thermo-oxidant is BF₃-pyridine, known to be both a mild oxidant²⁵ and a common impurity in cPPA which results in lowered polymer thermal stability²⁰.

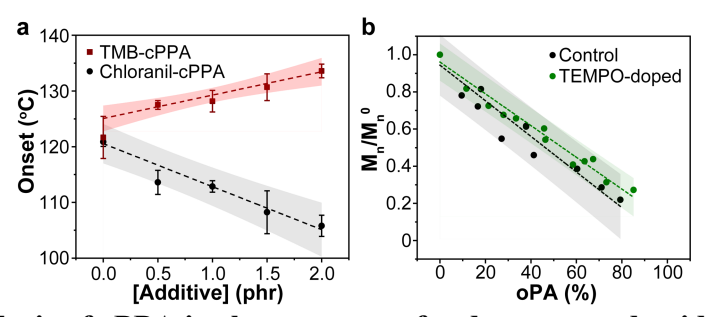


Figure 2. Thermolysis of cPPA in the presence of reductants and oxidants: (a) change in degradation onset temperature during 5 °C/min dynamic TGA scans of cPPA thin films as a function of 1,3,5-trimethoxybenzene (TMB) and p-chloranil concentration, phr = parts per hundred resin (b) evolution of molecular weight (M_n) as a function of conversion during thermolysis of cPPA thin films containing 2 phr TEMPO. In each plot, error bands and error bars represent 95% confidence; plotted points in (a) represent the average of three measurements.

Though it is not possible to determine if the BF₃-pyridine in cPPA is the operative oxidant, we can conclusively establish whether SET is the primary mode of thermolytic cPPA depolymerization. This SET triggering mechanism further predicts that electron donors, such

as 1,3,5-trimethoxybenzene (TMB, $E_{ox} = 1.539$ V vs SCE)²⁶, will inhibit the thermal degradation of cPPA. As shown in **Figure 2a**, addition of TMB to cPPA films results in a material with a higher degradation onset temperature. The onset of polymer degradation measured during dynamic TGA experiments varied linearly with TMB concentration. GPC analysis of the cPPA films during thermolysis in the presence and absence TMB show no significant differences in M_n evolution in doped and undoped samples (**Supporting Info**). This result indicates that the inhibitory action of TMB occurs *before* the activation of cPPA chains, consistent with the SET triggering mechanism and inconsistent with purely radical or purely ionic thermolysis mechanisms.

The addition of TEMPO to cPPA is known to stabilize the polymer toward thermolysis. 20 This effect had previously been rationalized by trapping of radical chain ends by TEMPO. In contrast, the SET triggering hypothesis predicts that TEMPO inhibition is due to sacrificial oxidation of TEMPO ($E_{ox} = 0.50 \text{ V vs SCE}^{27}$). To probe the nature of TEMPO inhibition, we monitored by GPC the evolution of polymer molecular weight during the thermolytic depolymerization of cPPA films in the presence and absence of added TEMPO. If the stabilizing effect of TEMPO was due to radical trapping, i.e. the deactivation of reactive cPPA termini after a scission event, the change in M_n during depolymerization would follow a non-linear trend²⁸, generating low molecular weight chains at low conversion. Instead, M_n of cPPA samples without TEMPO and with 2 phr added TEMPO followed statistically similar linear trends during depolymerization, with no observable low M_n species at low conversion (Figure 2b). This trend indicates that the stabilizing effect of TEMPO is not due to radical trapping, but rather suggests that TEMPO inhibits SET-activation of the polymer chain. These results exclude a homolytic thermal depolymerization mechanism and further support the SET-triggering hypothesis.

Having established a novel SET triggering mechanism as the primary thermal depolymerization pathway for cPPA, we were interested in the application of SET chemistry to develop photodegradable monolithic materials using photoinduced single electron transfer. Toward this end, we first investigated the photodepolymerization of cPPA by the photooxidant NMAPF₆²⁹ in solution (**Figure 3a**). A solution of NMAPF₆ (0.35 mM) and cPPA (20 mg/mL) in dichloromethane- d_2 was prepared. Photolysis at 375 nm (0.1 Wcm⁻²) resulted in the complete depolymerization of cPPA within four minutes. Depolymerization was confirmed by both GPC and ¹H NMR (**Figure 3b** and **3c**, respectively). The high molecular weight polymer peak at a retention time of 25 minutes in the pre-photolysis GPC trace is completely absent after UV exposure. Additionally, only resonances corresponding to cPPA and residual dichloromethane are visible by ¹H NMR (CD₂Cl₂, 60 MHz) before photolysis, while only oPA resonances (in addition to residual dichloromethane) are observed post-photolysis. Control samples that were kept in the dark and samples that were exposed to 0.1 Wcm⁻² 375 nm light in the absence of NMAPF₆ did not degrade appreciably over the same time period (**Supporting Information**). These results clearly demonstrate that photoinduced SET is an effective depolymerization trigger for cPPA.

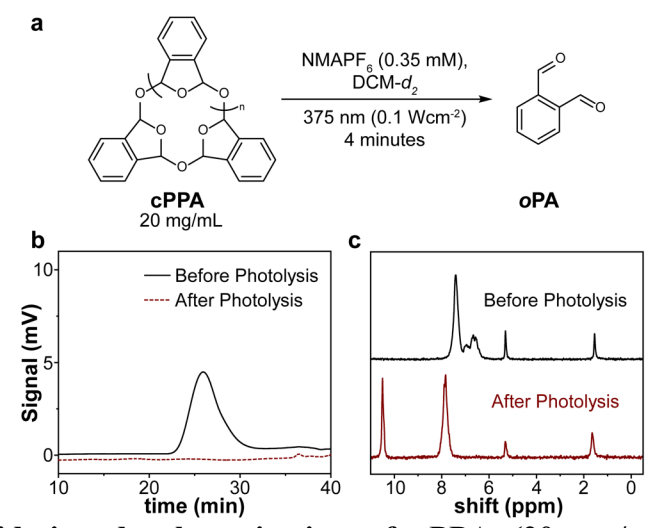


Figure 3. Photooxidative depolymerization of cPPA (20 mg/mL) by NMAPF₆ in dichloromethane solution: (a) reaction scheme; (b) gel permeation chromatography refractive index detection traces showing the presence and absence of high molecular weight polymer before and after photolysis, respectively; and (c) ¹H NMR of the reaction mixture before and

after photolysis, showing complete conversion to the monomer, oPA. ¹H NMR was collected at 60 MHz in dichloromethane- d_2 .

Having demonstrated that photoinduced SET triggers cPPA depolymerization in the solution state, we sought to investigate its application to solid-state depolymerization. To probe the utility of SET triggering in the solid state, we blended cPPA with NMAPF₆ in dichloromethane solution and drop cast to produce 100 µm thick films. Thin films with no added NMAPF₆ were clear and colorless and did not visibly degrade upon exposure to UV light (**Figure 4a-b**). Thin films doped with NMAPF₆, in contrast, were vibrant yellow and visibly degraded, forming a purple gel, when exposed to UV light (**Figure 4c-d**).

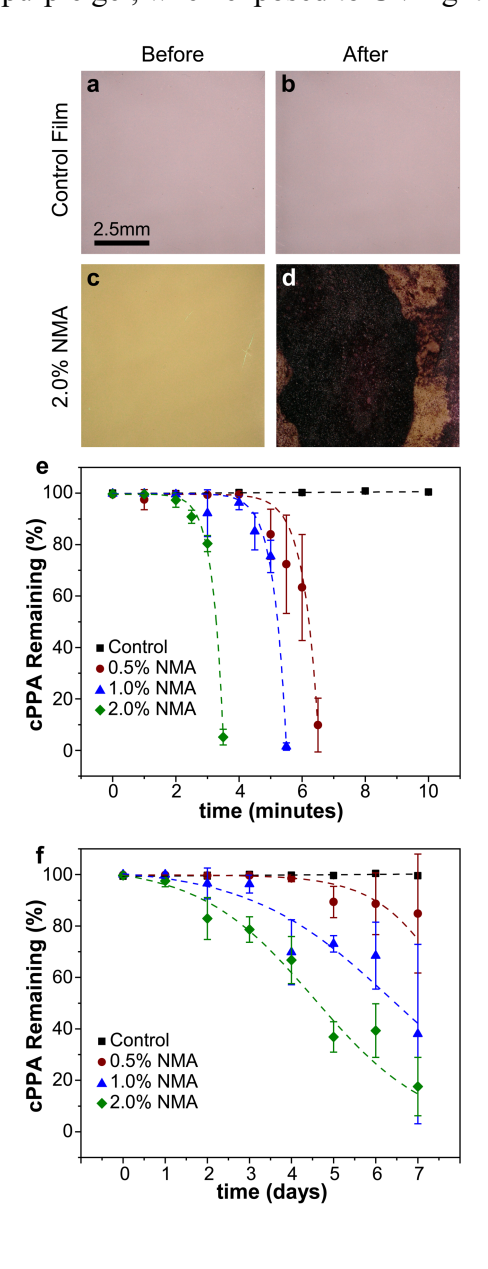


Figure 4. Controlled depolymerization of cPPA thin films by photochemical SET triggering at ambient temperature: micrographs of control cPPA films before and after exposure to UV light (a, b) and cPPA films with 2 mol% NMAPF₆ before and after exposure to UV light (c, d); depolymerization of cPPA thin films as monitored by 1 H NMR (60 MHz, DCM- d_2) during 375 nm UV irradiation at 0.1 Wcm⁻² with curves fit to an exponential function (e); and depolymerization of cPPA thin films in ambient room light as monitored by 1 H NMR (60 MHz, DCM- d_2) with curves fit to a logistic function (f). Each plotted point is the average of three measurements, and error bars represent 95% confidence.

The kinetics of film depolymerization were monitored by ¹H NMR during irradiation of thin films at 375 nm (0.1 Wcm⁻²) (see supporting information for data and analysis). Upon UV excitation, films rapidly depolymerized, with *o*PA as the only product visible by ¹H NMR. The rate of depolymerization was highly dependent on the loading of NMAPF₆ in the thin film. **Figure 4e** demonstrates the NMA dose dependence of cPPA depolymerization kinetics in samples with 0.5, 1.0, and 2.0 mol% NMAPF₆. Samples with no added NMAPF₆ did not degrade upon UV exposure, while those with 0.5, 1, and 2 mol % NMAPF₆ completely depolymerized within 6.5, 5.5, and 3.5 minutes, respectively. Importantly, NMAPF₆-doped samples that were not exposed to UV light did not depolymerize to any observable degree over the course of one week (**Supporting Information**). These results indicate that the SET-triggering process is facile in solid cPPA matrices.

Ambient room lighting was also sufficient to degrade the NMAPF₆-doped cPPA films. **Figure 4f** shows the depolymerization of thin films as a function of time at various photocatalyst loadings. At 2 mol % NMAPF₆, nearly quantitative conversion to monomer was observed after one week in ambient room lighting. Control samples without added NMAPF₆ did not degrade during the course of the experiment (**Figure 5f**), nor did NMAPF₆-doped cPPA films which were kept in the dark during the same period of time (**Supporting Information**). cPPA samples with lower loadings of NMAPF₆ (i.e. 0.5, 1.0 mol %) are expected to continue degrading if left under ambient lighting. This NMAPF₆ dose dependence provides a method by which to tune the rate of material degradation for various desired lifetimes.

While photodegradable thin films have been demonstrated previously by the creative application of photoacid generators (PAGS)^{6,30}, the thermal decomposition of PAGs precludes their use in the manufacture of monolithic photodegradable materials^{31,32}, which generally requires extended time at elevated temperature for melt processing. Thermally stable organic photooxidants present a promising tool for the manufacture of monolithic, photodegradable engineering plastics. Bulk material samples were fabricated following our previously reported procedure²⁰. Briefly, cPPA was solvent-blended in dichloromethane with a plasticizer (diphenylphthalate, 40-60 phr) and a photooxidant (NMAPF₆, 1 mol %) and drop cast in a dark enclosure to exclude ambient light. After 24 hours, the blended films were pulverized, and the resultant powder was used as a feedstock for thermoforming. Type V dog-bone samples (ASTM standard D638) were fabricated by hot-pressing the cPPA-NMAPF₆-DPP feedstock at 90 °C, 10 MPa for 5 minutes. The resultant monolithic materials were high-quality, optically transparent thermoplastics with an average storage modulus of 1.8 GPa, as measured by dynamic mechanical analysis (DMA) (Supporting Information).

To study photooxidative depolymerization of bulk polymers, the mechanical integrity of cPPA samples (thickness = $500 \mu m$) was measured by DMA during exposure to UV light. Optical images of a cPPA-NMAPF₆-DPP sample during UV irradiation at 0.35 Wcm^{-2} in the DMA instrument are shown in **Figure 5a-c**. The bulk material completely degrades in the irradiated area, resulting in a viscous liquid composed of monomer, plasticizer, and the photooxidant by-products. Unexposed and under-exposed regions remained visibly unaffected. As shown in **Figure 5d** the rate of material degradation is controlled by irradiation intensity. Bulk samples were monitored in the dark for a 300 second pre-exposure period to obtain a baseline stiffness, at which point the UV light source (375 nm) was turned on. Samples exposed to 0.1, 0.15, and 0.2 Wcm⁻² UV irradiation rapidly lost mechanical integrity, failing under tension within 600, 300, and 200 seconds, respectively. Samples that were not exposed to UV

light maintained their original stiffness throughout the experiment. Control samples without NMAPF₆ did not undergo significant change on exposure to equivalent UV irradiation (**Supporting Information**).

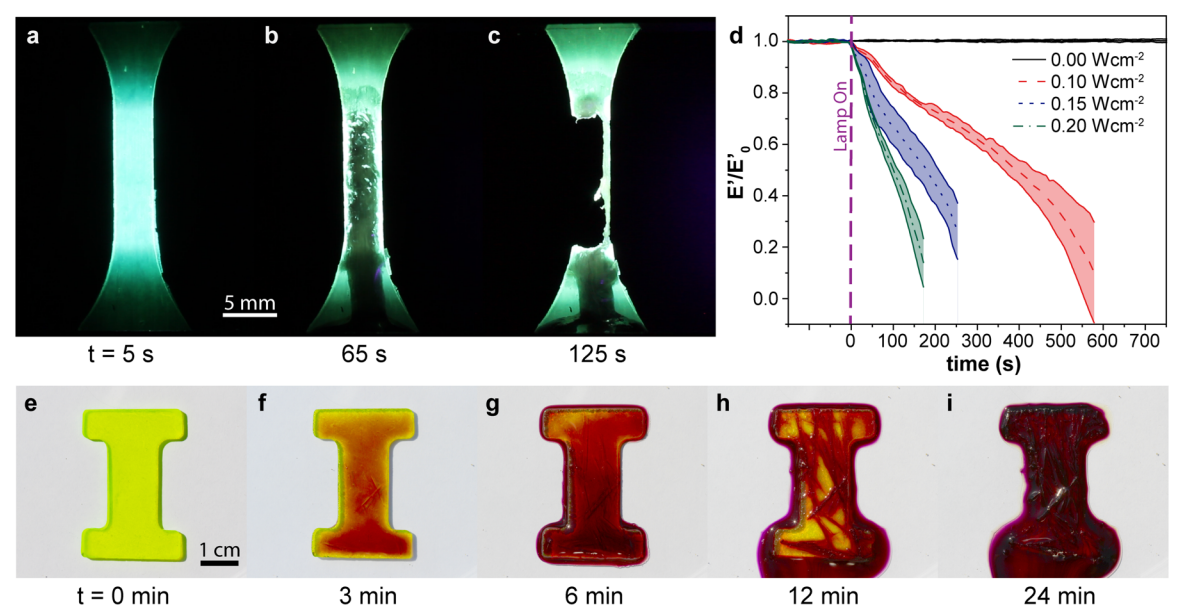


Figure 5. Controlled depolymerization of bulk cPPA samples by photochemical SET triggering: (a-c) Photographs of a cPPA-NMAPF₆ dog bone under 375 nm radiation (0.35 Wcm⁻²) at 5, 65, and 125 s, showing physical destruction of the polymer matrix. (d) Normalized E' of NMAPF₆-doped cPPA dog bones during photolysis at 375 nm at varying light intensities. Samples were monitored in the absence of light for 300 s, at which point the lamp was turned on. Each curve is an average of 3 samples, and error bands represent 95% confidence. (e-i) Bulk cPPA-NMAPF₆ degrading in sunlight on a sunny day in August in Champaign, IL, USA, over the span of 25 minutes. UV intensity during sunlight photodegradation was measured at 30 mWcm⁻², and the outdoor temperature was 24.5 °C.

Finally, the efficacy of SET-triggering for applications in environmental degradation was tested. Using the above thermoforming procedure, an I-shaped monolithic solid was manufactured (thickness = 2.0 mm). The sample was exposed to solar radiation (measured light intensity = 30 mWcm⁻²) and photographed at regular intervals (**Figure 5e-i**) on a white cardstock background. After 3 minutes of exposure to sunlight, the sample discolored along its surface. Within 6 minutes, viscous liquid had begun to pool around the sample. After 12 minutes of exposure, large, needle-like crystals appeared, indicating the formation of the crystalline monomer, *o*PA. Within 24 minutes of sunlight exposure, no visible polymer

remained. By using the novel SET triggering mechanism, we have successfully produced a sunlight-degradable monolithic material.

We have presented for the first time a transient polymer which undergoes rapid chain unzipping depolymerization to its constituent monomer following a single electron transfer trigger. SET triggering is achieved through multiple modes and was realized in both thermal and photochemical depolymerization of cyclic poly(phthalaldehyde). The collection of evidence presented here supports the mechanistic hypothesis of SET activation and subsequent mesolytic cleavage. This mechanism was used to tune the thermal stability of cPPA by the addition of oxidants and reductants. Additionally, photooxidation of cPPA using NMAPF₆ was demonstrated as an effective method of depolymerization in solution and in thin films. Finally, monolithic solids comprised of cPPA, diphenylphthalate, and NMAPF₆ were fabricated. These photooxidant-doped bulk solids were shown to exhibit desirable mechanical properties (E' = 1.8 GPa), and to respond rapidly to applied UV light, degrading completely into the corresponding monomer. Additionally, it was shown that the monolithic cPPA materials fully degraded to monomer within 25 minutes of sunlight exposure.

Given the ease with which cPPA depolymerizes by frequently encountered stimuli, it is unlikely to serve as a candidate to mitigate the environmental burden of single use plastics. Nonetheless, as a bulk engineering plastic that rapidly depolymerizes via photoredox catalysis, the chemical concepts presented here may inspire the development of new transient packaging. Even in its present state the applications for cPPA are evident, such as in the manufacture of transient delivery systems, and environmental sensing applications. For examples, it is conceivable that SET-triggered cPPA is well-suited for use in the manufacture of air gliding vehicles that deliver critical supplies and subsequently vanish by programmable transience, leaving no trace of the device. Most importantly, this work demonstrates a novel mode of SET-triggered transience and raises the prospect of SET as a depolymerization mechanism in a

potentially broad range of polymers. Thus, SET triggering of transient polymers is viewed as a promising area for future exploration.

Methods

General

All materials were purchased from Sigma-Aldrich and used without further purification unless otherwise noted. *Ortho*-Phthalaldehyde (*o*PA) was purchased from Oakwood Chemical and purified via vacuum distillation (0.1 torr, 90 °C). Poly(tetrafluoroethylene) petri dish liners were purchased from Welsh Fluorocarbon Inc. Ultra-high-molecular-weight polyethylene substrates were purchased from McMaster Carr. All prepared thin films were stored at -20 °C until use.

Analytical Gel Permeation Chromatography (GPC) was performed using a Waters 1515 isocratic HPLC pump and Waters 2707 96-well autosampler, equipped with a Waters 2414 refractive index detector and 4 Waters HR Styragel Column (7.8×300 mm, HR1, HR3, HR4, and HR5) in THF at 30 °C. The GPC system was calibrated using monodisperse polystyrene standards.

Thermogravimetric analysis (TGA) was performed using a TA Instruments Q500 TGA under a nitrogen atmosphere (90 mL/min). Dynamic TGA traces were obtained during a 5 °C/min ramp after equilibration at 40 °C. TGA samples consisted of 3-5 mg of the analyte film in a platinum pan. ¹H NMR spectra were recorded on a Varian VXR 500 (500 MHz) or an NMReady-60 benchtop NMR (60 MHz) purchased from Nanalysis Scientific Corp. UV photodepolymerization was performed using a custom-made 375 nm LED assembled with a 375 nm LED equipped with an AR coated aspherical condenser lens and an AR coated biconvex focusing lens (75 mm focal length). All parts were purchased from Thor Labs and assembled manually. A Keyence VHX-5000 series digital microscope was used to visualize

photodegradation of cPPA thin films. A Canon EOS 7D camera equipped with a 100 mm macro lens from Canon was used to image photodegradation of cPPA bulk materials.

Synthesis of cyclic poly(phthalaldehyde)

Cyclic poly(phthalaldehyde) (cPPA) was prepared via the cationic polymerization of purified *o*PA using a Lewis acid catalyst, BF₃-EtO₂, according to a known procedure. All reactions were run in anhydrous dichloromethane at -78 °C. Briefly, 40 g of *ortho*-phthalaldehyde (300 mmol) was dissolved in 200 mL of anhydrous DCM (1.5 M). The solution was first cooled down to -78 °C for 2 minutes upon which 0.8 mL of BF₃-EtO₂ (6.5 mmol) was added to the reaction. The solution was stirred using a mechanical stirrer for 2 hours, at which point it had become highly viscous. The reaction was then quenched using 2 mL of pyridine and was stirred for an additional 2 hours. Finally, the reaction mixture was precipitated in 4 L of methanol. The precipitated polymer was dried via vacuum filtration for 1 hour and subsequently dried on hi-vac overnight to afford 36.5 g (92%) of a white solid. The polymer was stored at -20 °C until use.

¹H NMR (CD₂Cl₂, 500 MHz) δ 5.75-7.75 (br, 6 H). M_n = 250 kDa, Θ = 1.67.

Synthesis of N-methylacridinium iodide

N-methylacridinium iodide (NMAI) was synthesized according to literature procedure.³³ Briefly, a 100 mL oven dried round bottom flask was charged with a stir bar. 5.0 g of acridine (27.6 mmol) was dissolved in 20 mL DMF and was heated to 35 °C for 10 minutes.

3.4 mL iodomethane (55 mmol) was added into the reaction flask. The reaction flask was heated to 50 °C overnight under dry nitrogen. 100 mL of diethyl ether was added to the reaction mixture, and the precipitated solid was then isolated via vacuum filtration. The compound was dried on hi-vac overnight to yield 6.6 g of material (74%) and was used without further purification.

¹H NMR (CD₂Cl₂, 500 MHz) δ 10.02 (s, 0.95 H), 8.67 (d, 2 H), 8.61 (dd, 1.96 H), 8.47 (ddd, 1.99 H), 8.02 (ddd, 1.97 H), 5.00 (s, 3.16 H).

Synthesis of N-methylacridinium hexafluorophosphate

1.09 g of NMAI (3.3 mmol) was dissolved in 120 mL of water and a 20 mL aqueous potassium hexafluorophosphate (1.22 g, 6.6 mmol) solution was added. A yellow precipitate formed immediately. The solution was stirred for 30 minutes and the precipitate was isolated via vacuum filtration. The precipitate was washed with 3×50 mL water and was then dried under vacuum overnight. The dried product purified via recrystallization in methanol, forming small needle-like crystals (253 mg, 28.6 % yield). The resulting compound was dried under vacuum and stored away from light.

 1 H NMR (CD₂Cl₂, 500 MHz) δ 9.77 (s, 0.98 H), 8.52 (ddd, 3.95 H), 8.45 (m, 1.99 H), 8.02 (ddd, 1.95 H), 4.87 (s, 3.13 H).

Solvent casting cPPA thin films

Free standing pristine cPPA thin films were prepared according to literature procedure. Procedure. Procedure PPA (100 mg) was dissolved in HPLC grade dichloromethane (3 mL). The solution was then cast into a 50 mm diameter PTFE-lined petri dish and allowed to dry for 24 hours in a light-free cardboard enclosure with solvent-saturated atmosphere. Films used in reductant and oxidant stability tests were doped with 0.5, 1.0, 1.5 and 2.0 mg of 1,3,5-trimethoxybenzene (TMB) or p-chloranil (pCA) before casting. Films used in trapping experiments were doped with 2.0 mg TEMPO or TMB before casting.

Photodegradable thin films were prepared by dissolving 300 mg cPPA in 5 mL of DCM along with a known amount of NMAPF₆ (0, 3.8, 7.7, and 15.5 mg for 0, 0.5, 1.0, and 2.0 mol% NMAPF₆ loading, respectively). cPPA-NMAPF₆ solutions were cast into 50 mm diameter PTFE-lined dishes as above.

cPPA trapping experiments

Small sections of cPPA thin films were cut and weighed out (~5 mg). The films were placed into the bottom of scintillation vials. The vials were then immersed in an oil bath that was kept at 100 °C. The vials were removed at 5-minute intervals and the repolymerization qunched using an ice bath. The vial contents were dissolved in 0.25 ml of THF and analyzed by GPC. The GPC traces were normalized by the initial mass of the film, and conversion was determined via the ratio of the normalized area of high molecular weight peaks (retention times between 20-35 minutes) of samples subjected to thermolysis and a control sample that was not subjected to thermolysis.

The trends of Mn vs. conversion for samples doped with TMB and with TEMPO were compared against those of pristine cPPA films run at the same time using an F-test. The trends were not found to be statistically different at the 0.05 significance level.

Solution state photolysis of cPPA

A solution of cPPA (20 mg/mL) in DCM- d_2 was transferred to a 1 cm UV quartz cell, and a stir bar was added. A separate solution containing cPPA (20mg/mL) and NMAPF₆ (0.35mM) was similarly prepared. Both solutions were stirred and irradiated with a 375 nm LED for 4 minutes. Before and after photolysis, the crude reaction mixtures were analyzed by 1 H NMR. After photolysis, the solvent was evaporated via a rotary evaporator, and the residue was dissolved in THF and analyzed via gel permeation chromatography (GPC). In the absence of NMAPF₆, no significant change was observed in either 1 H NMR or GPC. In the presence of NMAF₆, both 1 H NMR and GPC indicate complete conversion of cPPA to oPA over the course of four minutes.

Thin film photolysis of cPPA

Pristine cPPA and NMAPF₆-doped cPPA films were cut into small square sections (0.5 cm x 0.5 cm) and were placed into scintillation vials. A 375 nm UV LED was positioned above the square samples at the focal point of the light source. The films were then irradiated for a

given time (0-10 minutes). Following UV exposure, the irradiated films were dissolved in DCM- d_2 and characterized using ¹H NMR (60 MHz, DCM- d_2). The conversion of polymer to monomer was monitored by comparing the ratio of the oPA aldehyde resonance peak (10.5 pm) and the phenyl resonance peaks of both oPA and cPPA (ca. 8-6 ppm). The percent of cPPA in each film was calculated according to the following equations:

(1)
$$\% cPPA = \frac{[cPPA]_{rel}}{[cPPA]_{rel} + [oPA]_{rel}} \times 100\%$$

(2)
$$[cPPA]_{rel} = [I_{8-6} - I_{10.5} \times C_f \times 2] \times \frac{1}{6}$$

(3)
$$[oPA]_{rel} = [I_{10.5} \times C_f] \times \frac{1}{2}$$

Where $I_{I0.5}$ is the integral of the resonance at 10.5 ppm, corresponding to the aldehyde proton of oPA; I_{8-6} is the integral of the broad resonance in the 8-6 ppm region, which corresponds to all six proton resonances of cPPA and the four aryl protons of oPA. To account for the incomplete relaxation of the aldehydic protons of oPA, a correction factor (C_f) of 1.26 was introduced into the calculation. Equation 1 shows the general calculation for the percent of cPPA in a sample. In Equation 2, the relative concentration of cPPA is calculated by subtracting the integral contribution in the 6-8 ppm region from oPA (2 times $I_{10.5}$, with a correction factor), normalized by the proton count (6). Equation 3 calculates the relative concentration of oPA by correcting $I_{10.5}$ and normalizing by the proton count (2).

Ambient light cPPA thin film degradation

Pristine cPPA and NMAPF₆-doped cPPA films were cut into small square sections (0.5 cm x 0.5 cm) which were placed into scintillation vials. The samples were exposed to ambient light by placing them inside of a fume hood (ambient light intensity = 6 μ Wcm⁻²) and leaving them for a given amount of time (0-7 days). Following ambient light exposure, the irradiated films were dissolved in DCM- d_2 and characterized using ¹H NMR. The conversion of polymer to monomer was monitored by ¹H NMR using the method described in the *Thin Film Photolysis* section above.

Fabrication of cPPA monoliths

cPPA Feedstock Preparation

5.0 g of cPPA and diphenylphthalate (2.0 or 3.0 g for dog-bone feedstock and I-shaped monolith feedstock, respectively) were dissolved in HPLC grade dichloromethane (40 mL). To prepare the photooxidant-doped feedstock 127 mg (1 mol % with respect to *o*PA repeat unit) NMAPF₆ was added to the solution. Solutions were then tape cast onto an ultra-high-molecular-weight polyethylene substrate in the dark. Film thickness (200 μm) was set with a high precision film applicator. Films were left in a dichloromethane-saturated environment for 24 h. This process generated a free-standing film which was then pulverized into a powder feedstock using a coffee grinder.

cPPA Monolith Preparation

300 mg of cPPA feedstock prepared above (with or without added NMAPF₆) were placed into an aluminum dogbone mold (ASTM Standard D638 Type V). The filled mold was then preheated at 90 °C for 5 minutes. Samples were then pressed at 10 MPa and 90 °C for 5 minutes. The mold was cooled down (10 °C/min) to room temperature, and the dog-bones (500 µm thick) were removed from the mold. The same process was used to produce the "I" shaped monoliths using 1.5 g of cPPA feedstock.

Storage Modulus Determination

Dynamic mechanical analysis (DMA) was performed using a TA Instruments RSA III. Both pristine cPPA and NMAPF6-doped cPPA samples were loaded onto the DMA using thin film grips provided by TA Instruments. The gauge length was set to 8 mm. Oscillatory load was applied at 10 Hz and 0.1 % strain amplitude at 20 °C. The storage modulus of three samples was measured for both pristine cPPA samples and NMAPF6-doped samples. The average storage moduli of pristine and NMAPF6-doped samples were 1.54±0.10 and 1.78±0.11 GPa, respectively.

Dynamic mechanical analysis of cPPA during photodegradation

Pristine cPPA and NMAPF₆-doped cPPA specimens were loaded onto the DMA, and the gauge length was set to 25 mm. Oscillatory loading was applied at 10 Hz and 0.1 % strain amplitude at 20 °C. The samples were first characterized in the dark for a 300 second preexposure period after which the UV light source (0.1, 0.15, or 0.2 Wcm⁻²) was turned on. Specimens were tested until they failed in tension. Degradation was monitored optically with a Canon EOS 7D camera equipped with a 100 mm macro lens.

Sunlight depolymerization of cPPA

"I" shaped cPPA monoliths prepared above were placed on a glass petri dish and placed outside on a sunny day, September 6th, 2019 in Urbana, Illinois. Photographs of the specimens were taken at 5 second intervals for 25 minutes. The UV intensity during sunlight photodegradation was measured to be 30 mWcm⁻², and the outdoor temperature was 30.5 °C. The NMAPF-doped cPPA sample showed complete degradation after 24 minutes of exposure whereas the pristine cPPA sample showed no visual signs of degradation.

Associated Content

Supporting information. Representative UV-Vis and ¹H NMR spectra; representative thermogravimetric data; additional control experiment data.

Video files. Videos of (1) UV-triggered depolymerization of a doped cPPA dog-bone and (2) sunlight-triggered depolymerization of doped cPPA monolith with an un-doped control.

Acknowledgments

This manuscript is dedicated to the late Prof. Scott White, a constant mentor, inspiration, and friend. The authors gratefully acknowledge the support of the National Science Foundation through a Phase I Center for Chemical Innovation Grant (CHE-1740597). E.M.L

thanks the Arnold and Mabel Beckman Foundation for financial support. The authors thank Dorothy Loudermilk for assistance with graphics. The authors also thank the Beckman Institute for Advanced Science and Technology for the facilities and support to conduct this research.

Author Contributions

J.S.M. and N.S. directed this research. J.S.M. and A.M.F. conceived the idea. O.D., E.M.L., D.G.I., B.S., and A.M.F. performed the experiments. All authors participated in writing the manuscript.

Competing Interests

The authors declare no competing interests.

References

- (1) Brian, N. T. A Review of Melt Extrusion Additive Manufacturing Processes: I. Process Design and Modeling. *Rapid Prototyp. J.* **2014**, *20* (3), 192–204.
- (2) Marsavina, L.; Cernescu, A.; Linul, E.; Scurtu, D.; Chirita, C. Experimental Determination and Comparison of Some Mechanical Properties of Commercial Polymers. *Mater. Plast.* 2010, 47, 45–89.
- (3) Kondo, H.; Tanaka, T.; Masuda, T.; Nakajima, A. Aging Effects in 16 Years on Mechanical Properties of Commercial Polymers (Technical Report). *Pure and Applied Chemistry*. 1992, p 1945.
- (4) Eriksen, M.; Lebreton, L. C. M.; Carson, H. S.; Thiel, M.; Moore, C. J.; Borerro, J. C.; Galgani, F.; Ryan, P. G.; Reisser, J. Plastic Pollution in the World's Oceans: More than 5 Trillion Plastic Pieces Weighing over 250,000 Tons Afloat at Sea. *PLoS One* 2014, 9 (12), e111913.

- (5) Joo, W.; Wang, W.; Mesch, R.; Matsuzawa, K.; Liu, D.; Willson, C. G. Synthesis of Unzipping Polyester and a Study of Its Photochemistry. *J. Am. Chem. Soc.* **2019**, *141* (37), 14736–14741.
- (6) Hernandez, H. L.; Kang, S.-K.; Lee, O. P.; Hwang, S.-W.; Kaitz, J. A.; Inci, B.; Park,
 C. W.; Chung, S.; Sottos, N. R.; Moore, J. S.; et al. Triggered Transience of Metastable
 Poly(Phthalaldehyde) for Transient Electronics. *Adv. Mater.* 2014, 26 (45), 7637–7642.
- (7) Sagi, A.; Weinstain, R.; Karton, N.; Shabat, D. Self-Immolative Polymers. *J. Am. Chem. Soc.* **2008**, *130* (16), 5434–5435.
- (8) Romero, N. A.; Nicewicz, D. A. Organic Photoredox Catalysis. *Chem. Rev.* 2016, 116(17), 10075–10166.
- (9) Zhang, N.; Samanta, S. R.; Rosen, B. M.; Percec, V. Single Electron Transfer in Radical Ion and Radical-Mediated Organic, Materials and Polymer Synthesis. *Chem. Rev.* 2014, 114 (11), 5848–5958.
- (10) Pross, A. The Single Electron Shift as a Fundamental Process in Organic Chemistry:
 The Relationship between Polar and Electron-Transfer Pathways. *Acc. Chem. Res.* 1985, 18 (7), 212–219.
- (11) Weinberg, N. L.; Weinberg, H. R. Electrochemical Oxidation of Organic Compounds. *Chem. Rev.* **1968**, *68* (4), 449–523.
- (12) Lopez Hernandez, H.; Takekuma, S. K.; Mejia, E. B.; Plantz, C. L.; Sottos, N. R.; Moore, J. S.; White, S. R. Processing-Dependent Mechanical Properties of Solvent Cast Cyclic Polyphthalaldehyde. *Polymer (Guildf)*. 2019, 162, 29–34.
- (13) Schwartz, J. M.; Phillips, O.; Engler, A.; Sutlief, A.; Lee, J.; Kohl, P. A. Stable, High-Molecular-Weight Poly(Phthalaldehyde). *J. Polym. Sci. Part A Polym. Chem.* **2017**, *55* (7), 1166–1172.

- Kaitz, J. A.; Diesendruck, C. E.; Moore, J. S. End Group Characterization of Poly(Phthalaldehyde): Surprising Discovery of a Reversible, Cationic
 Macrocyclization Mechanism. J. Am. Chem. Soc. 2013, 135 (34), 12755–12761.
- (15) Lloyd, E. M.; Lopez Hernandez, H.; Feinberg, A. M.; Yourdkhani, M.; Zen, E. K.; Mejia, E. B.; Sottos, N. R.; Moore, J. S.; White, S. R. Fully Recyclable Metastable Polymers and Composites. *Chem. Mater.* 2019, 31 (2), 398–406.
- (16) Park, C. W.; Kang, S.-K.; Hernandez, H. L.; Kaitz, J. A.; Wie, D. S.; Shin, J.; Lee, O.
 P.; Sottos, N. R.; Moore, J. S.; Rogers, J. A.; et al. Thermally Triggered Degradation of Transient Electronic Devices. *Adv. Mater.* 2015, 27 (25), 3783–3788.
- (17) Diesendruck, C. E.; Peterson, G. I.; Kulik, H. J.; Kaitz, J. A.; Mar, B. D.; May, P. A.; White, S. R.; Martínez, T. J.; Boydston, A. J.; Moore, J. S. Mechanically Triggered Heterolytic Unzipping of a Low-Ceiling-Temperature Polymer. *Nat. Chem.* **2014**, *6*, 623.
- (18) Lutz, J. P.; Davydovich, O.; Hannigan, M. D.; Moore, J. S.; Zimmerman, P. M.;
 McNeil, A. J. Functionalized and Degradable Polyphthalaldehyde Derivatives. *J. Am. Chem. Soc.* 2019, *141* (37), 14544–14548.
- (19) Tsuda, M.; Hata, M.; Nishida, R.; Oikawa, S. Acid-Catalyzed Degradation Mechanism of Poly(Phthalaldehyde): Unzipping Reaction of Chemical Amplification Resist. *J. Polym. Sci. Part A Polym. Chem.* **1997**, *35* (1), 77–89.
- (20) Feinberg, A. M.; Hernandez, H. L.; Plantz, C. L.; Mejia, E. B.; Sottos, N. R.; White, S. R.; Moore, J. S. Cyclic Poly(Phthalaldehyde): Thermoforming a Bulk Transient
 Material. ACS Macro Lett. 2018, 7 (1), 47–52.
- (21) Boyd, J. W.; Schmalzl, P. W.; Miller, L. L. Mechanism of Anodic Cleavage of Benzyl Ethers. *J. Am. Chem. Soc.* **1980**, *102* (11), 3856–3862.
- (22) Rathore, R.; Kochi, J. K. Radical-Cation Catalysis in the Synthesis of

- Diphenylmethanes via the Dealkylative Coupling of Benzylic Ethers. *J. Org. Chem.* **1995**, *60* (23), 7479–7490.
- (23) Carlotti, B.; Del Giacco, T.; Elisei, F. Competition of C–H and C–O Fragmentation in Substituted p-Methoxybenzyl Ether Radical Cations Generated by Photosensitized Oxidation. *Photochem. Photobiol. Sci.* **2013**, *12* (3), 489–499.
- (24) Sasaki, K.; Kashimura, T.; Ohura, M.; Ohsaki, Y.; Ohta, N. Solvent Effect in the Electrochemical Reduction of P-Quinones in Several Aprotic Solvents. *J. Electrochem. Soc.* **1990**, *137* (8), 2437–2443.
- (25) Chénard, E.; Sutrisno, A.; Zhu, L.; Assary, R. S.; Kowalski, J. A.; Barton, J. L.; Bertke, J. A.; Gray, D. L.; Brushett, F. R.; Curtiss, L. A.; et al. Synthesis of Pyridine–and Pyrazine–BF3 Complexes and Their Characterization in Solution and Solid State. *J. Phys. Chem. C* **2016**, *120* (16), 8461–8471.
- (26) Luo, P.; Feinberg, A. M.; Guirado, G.; Farid, S.; Dinnocenzo, J. P. Accurate Oxidation Potentials of 40 Benzene and Biphenyl Derivatives with Heteroatom Substituents. *J. Org. Chem.* **2014**, *79* (19), 9297–9304.
- (27) Israeli, A.; Patt, M.; Oron, M.; Samuni, A.; Kohen, R.; Goldstein, S. Kinetics and Mechanism of the Comproportionation Reaction between Oxoammonium Cation and Hydroxylamine Derived from Cyclic Nitroxides. *Free Radic. Biol. Med.* 2005, 38 (3), 317–324.
- (28) Carothers, W. H. Polymers and Polyfunctionality. *Trans. Faraday Soc.* **1936**, *32* (0), 39–49.
- (29) Todd, W. P.; Dinnocenzo, J. P.; Farid, S.; Goodman, J. L.; Gould, I. R. Efficient Photoinduced Generation of Radical Cations in Solvents of Medium and Low Polarity. *J. Am. Chem. Soc.* 1991, 113 (9), 3601–3602.
- (30) Jiang, J.; Phillips, O.; Engler, A.; Vong, M. H.; Kohl, P. A. Photodegradable Transient

- Bilayered Poly(Phthalaldehyde) with Improved Shelf Life. *Polym. Adv. Technol.* **2019**, 30 (5), 1198–1204.
- (31) Spencer, T. J.; Kohl, P. A. Decomposition of Poly(Propylene Carbonate) with UV Sensitive Iodonium Salts. *Polym. Degrad. Stab.* **2011**, *96* (4), 686–702.
- (32) Yamato, H.; Asakura, T.; Matsumoto, A.; Ohwa, M. Novel Photoacid Generators for Chemically Amplified Resists. In *Proc.SPIE*; 2002; Vol. 4690.
- (33) Eberhard, J.; Peuntinger, K.; Fröhlich, R.; Guldi, D. M.; Mattay, J. Synthesis and Properties of Acridine and Acridinium Dye Functionalized Bis(Terpyridine) Ruthenium(II) Complexes. *European J. Org. Chem.* 2018, 2018 (20–21), 2682–2700.

For Table of Contents Only

